NINTH·EUROPEAN ROTORCRAFT FORUM

Paper No. 46

THE VIBRATORY AIRLOADING OF HELICOPTER ROTORS

W. E. HOOPER

Boeing Vertol Company
Philadelphia
USA

September 13-15, 1983

STRESA, ITALY

Associazione Industrie Aerospaziali

Associazione Italiana di Aeronautica ed Astronautica

THE VIBRATORY AIRLOADING OF HELICOPTER ROTORS

W. E. Hooper

Boeing Vertol Company
Philadelphia, USA

ABSTRACT

A survey has been made of all major wind tunnel and full-scale flight tests conducted over the last 29 years to examine the nature of the vibratory aerodynamic loading which causes helicopter vibration. Using computer generated surface plots, the present paper compares the airload distributions for rotors which have from 2 through 6 blades by presenting the data in identical plotting formats which allow comparisons of the effects of major parameters including blade number, blade/vortex proximities, propulsive force and forward speed.

By harmonically analyzing the data, it has been possible to show striking similarities between the vibration-causing higher harmonics of airloading on different rotor designs and in widely varying flight conditions. By selectively eliminating the lower harmonics, the predominant modes of vibratory forcing, to which all helicopter blades are subjected, are revealed.

1. INTRODUCTION

As part of a study to determine the nature of the airloading on rotor blades that causes helicopter vibration, a survey has been made of all published rotor blade pressure testing that has been conducted over the last 29 years starting with the NACA/Langley 2 bladed, 15 ft. dia. teetering model tested by Rabbott and Churchill up to the most recent testing of the Bell AH-1G by NASA/Ames (Table 1). An enormous volume of data are available in the public domain covering 2,3,4,5 and 6 bladed helicopters all with at least 50 pressure measurement points on the instrumented blades together with strain gages for flap and chordwise bending, and torsion.

	VEHICLE	BLADES	AGENCY	REF.	MFR	PRESSURE PU'S	OTHER INSTR.
NACA LANGLEY MODEL RABBOTT/CHURCHILL	15' DIA TEETERING W/T MODEL	2	NACA LANGLEY	NACA RM L56107 OCT 56	-	50 XDUCERS ALL DIFFERENTIAL 5 RADIAL STA 10 CHDWISE LOCATIONS	PITCH & FLAP ANGLE
DYNAMIC AIRLOADS (FLT TEST) AUG-OCT 1961	UH-1	2	USA TRC	TCREC TR 62-42 DEC 62	BELL	54 DIFF'L XDUCERS 6 STA. 11 @ 85% RADIUS	3 FLAP BENDING 4 CHORD 2 TORSION
H-34 FLIGHT TEST SCHIEHAN	H-34	4	NASA LANGLEY	NASA TM X-952 MAR 64	SIKORSKY	53 XDUCERS AT 7 RADIAL STA, 11 @ 85%	
FULL SCALE W/T (H-34) CORRELATED WITH THEORY RABBOTT/LIZAR/PAGLINO	H-34 56' DIA 16.4" CHD	4	USAAML AMES	USAAVLABS TR 66-31 JUL 66	SIKORSKY	56, 9 STA. 11 @ 85%	4 FLAP BENDING 4 CHORD BENDING 3 TORSION
DYNAMIC AIRLOADS (FLT TEST) PRUYN	CH-47A	2X 3	USAAVLABS	USAAVLABS TR 68-22A MAY 68	VERTOL	54 LOCATIONS 8 STA 11 @ 85%-2 ROTORS	8 FLAP BENDING 4 CHORD BENDING 2 TORSION 1 AXIAL
FLIGHT MEASUREMENT & CORRELATION BARTSCH	XH-51A 35' DIA	4	USAAVLABS	USAAVLABS TR 68-22A MAY 68	LOCKHEED	46 DIFF'L XDUCERS 7 STA, 7 CHDWISE, EXCEPT INBOARD	9 FLAP BENDING 4 CHORD BENDING 2 TORSION 1 PITCH LINK
S-61 FLIGHT TEST (COMPOUND) FENAUGHTY, BENO	HH-3A 62' DIA 660 FT/SEC	5	NASC	NASC SER 611493 JAN 70	SIKORSKY	29 LOCATIONS 16 ABSOLUTE (DUAL) 13 DIFF'L	7 FLAP BENDING 6 CHORD BENDING 2 TORSION 1 AXIAL TOT 89
CH-53 FLT TEST BENO	CH-53	6	NAVY	NASC SER 65593 JUN 70	SIKORSKY	34 ABSOLUTE & 10 DIFF'L ON BLADE 10 DIFF ON TAIL	3 HUB ACCELS 4 LOAD CELLS ON TAIL
AH-1G FLT TEST AERO & STRUCT LOAD SURVEY (1976)	AH-1G	2	ARMY	USAAMRDL TR76-39 FEB 77	BELL	130 ABSOLUTE 5 RADIAL STA	
AH-1G FLT TEST TIP AERO-ACOUSTIC TEST (1981)	AH-1G	2	NASA	(LATE '83)	BELL	188 ABSOLUTE	30 BENDING/TORSION 5 BLADE ACCELS 15 BOUNDARY LAYER

The main objectives of the study were to determine:

(a) the nature of the vibratory airloading occurring on helicopter blades, which leads to the n/rev vibratory forcing transmitted down the rotor shaft to the airframe.

(b) whether any consistent patterns emerge between blades of different designs, rotors having different numbers of blades, and forward flight characteristics such as speed, lift, and rotor propulsive force.

and (c) whether the vibratory airloading is adequately represented by today's analytical capabilities.

An early obstacle encountered was that many of the reports available today present the data in different formats, e.g. incremental tabulation of data (every 5°, 10° or 15°), data already transformed into harmonic coefficients, (using either positive or negative definitions) data from which the steady components have been separated from the vibratory components, etc. Initially, use was made of a surface plotting program to examine the data on a three dimensional polar plot format. For example, Figure 1 shows the

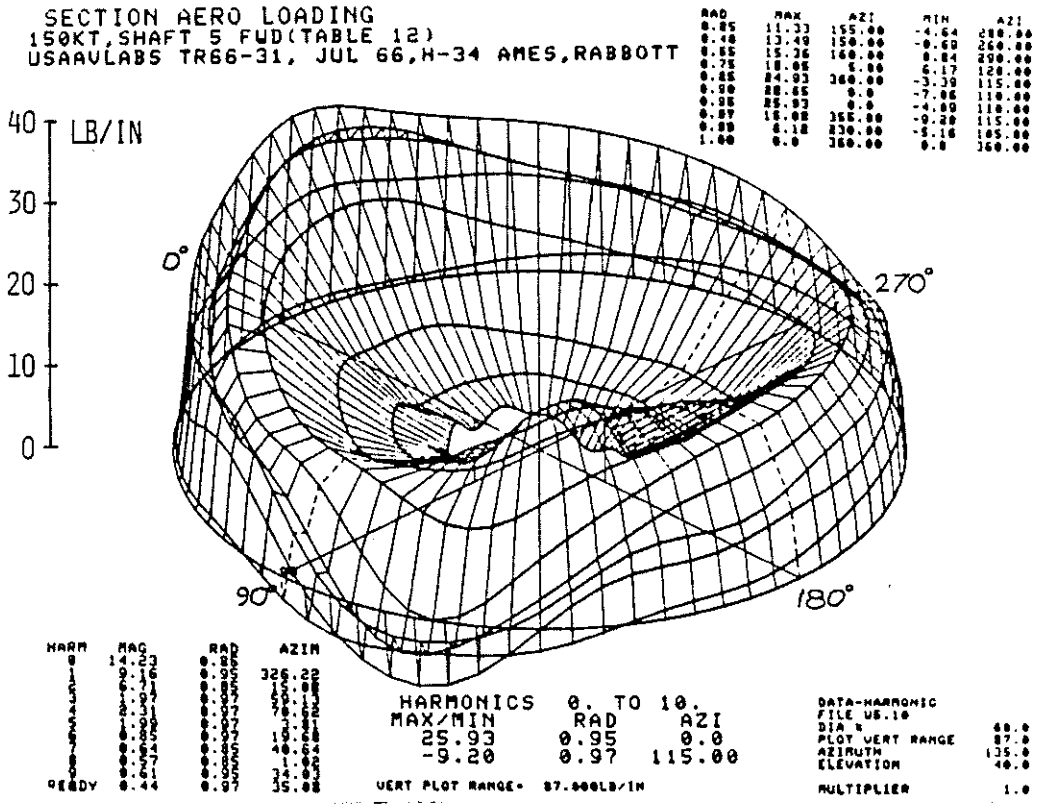

Fig. 1. Polar Surface Plot of H-34 Airloading

airloading distribution of the H-34 tested in the Ames tunnel in a propulsive condition at 150 kt. However, it was found that a more useful projection was obtained by developing the rotating blade motion into a linear motion much as if the blade was a wing (Figure 2). Comparison of these two figures shows that while the polar form conveys a physical impression of the data, more information can be deduced from the linear format of Figure 2 since every azimuth is viewed from the same perspective. The projection angles used in this example were retained for examination of other data. This particular example is for test data tabulated every 5° but it was found that when compared with data tabulated at 15° increments (e.g. flight test of the H-34) that much of the visual comparative value was lost. Accordingly, the surface plot program was modified to first perform a harmonic analysis of the test data up to 10 harmonics and then to reconstruct the raw data in 5° increments.

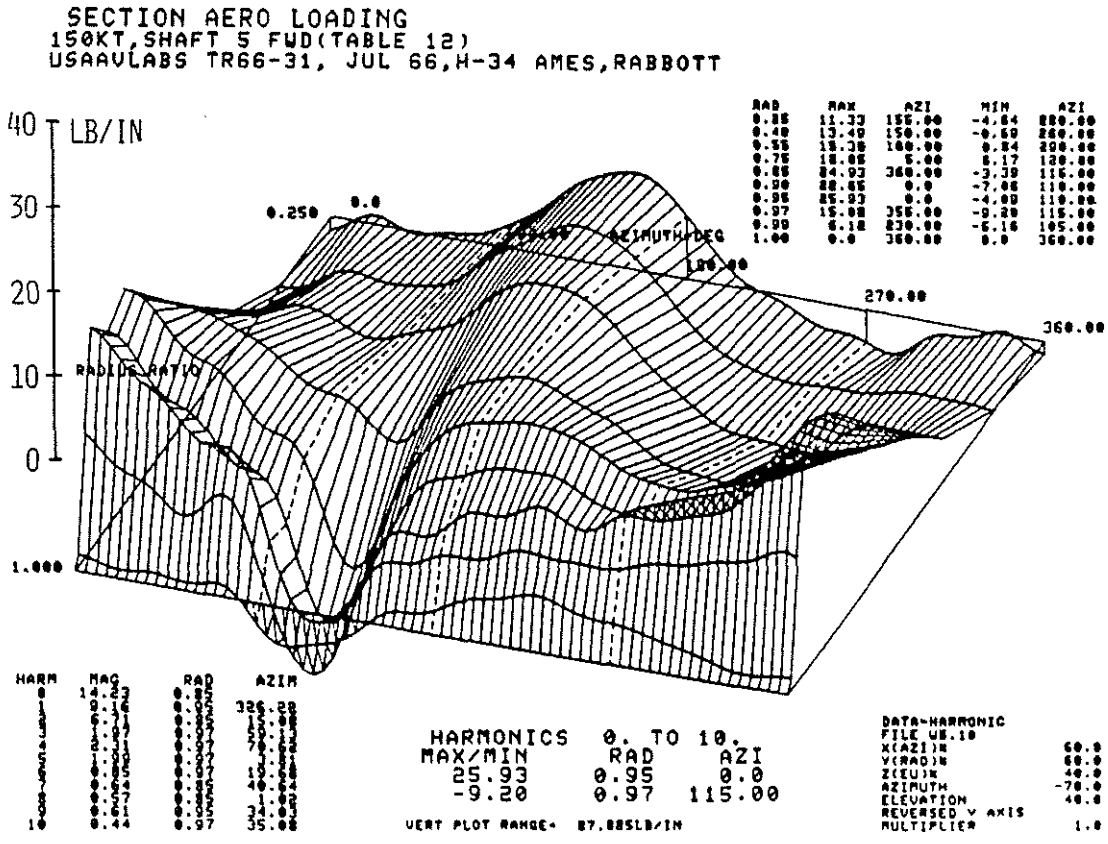

Fig. 2. Linear Surface Plot of H-34 Airloading

2. Harmonic Analysis

Since airloading harmonics 3, 4 and 5 are those that contribute to shaft transmitted vibration of a 4 bladed helicopter, all the test data were examined by plotting individual harmonics up to 5 in the cartesian surface format. It soon became apparent that -

a) The magnitude of the 3,4 and 5/Rev harmonics were similar for a particular test point (rather than reducing with increased order as might have been expected.)

and b) the phase of the harmonics at higher speeds varied little between widely different rotor designs.

An illustration of the constant term and the first 5 harmonics is given in Figure 3 for the H-34 wind tunnel case of Figures 1 & 2. The constant term shows a parabolic lift distribution as might be expected (with a minor anomaly near the tip.) The 1st harmonic component is unique in that the 1st harmonic airloads need to be in approximate moment balance about the hub for low steady shaft moment. In this case the upward inboard airload at 140° azimuth in the 2nd quadrant is balancing the downward airload at the tip, and the reverse is occurring in the 4th quadrant. Higher harmonics do not need to be in moment balance and the 2nd harmonic on the 4 bladed rotor can be seen to cancel itself across the disc. The 6.71 lb/in magnitude at the 85%radius accounts for the movement of rotor lift to the front and back of the disc at high forward speed. The 3rd, 4th and 5th harmonics all show essentially unchanging phase with radius (i.e. the peaks occur at the same azimuth at all radii). From this presentation of the data no major conclusion emerges as to the nature of the vibration causing the 3, 4, and 5/rev airloads since each harmonic maintains its magnitude around the disc. However, an examination of all the other data from the test program showed a surprising consistency in the phase of the 3, 4 or 5 harmonics. In this case note that all the harmonics have a minimum value near 120° azimuth.

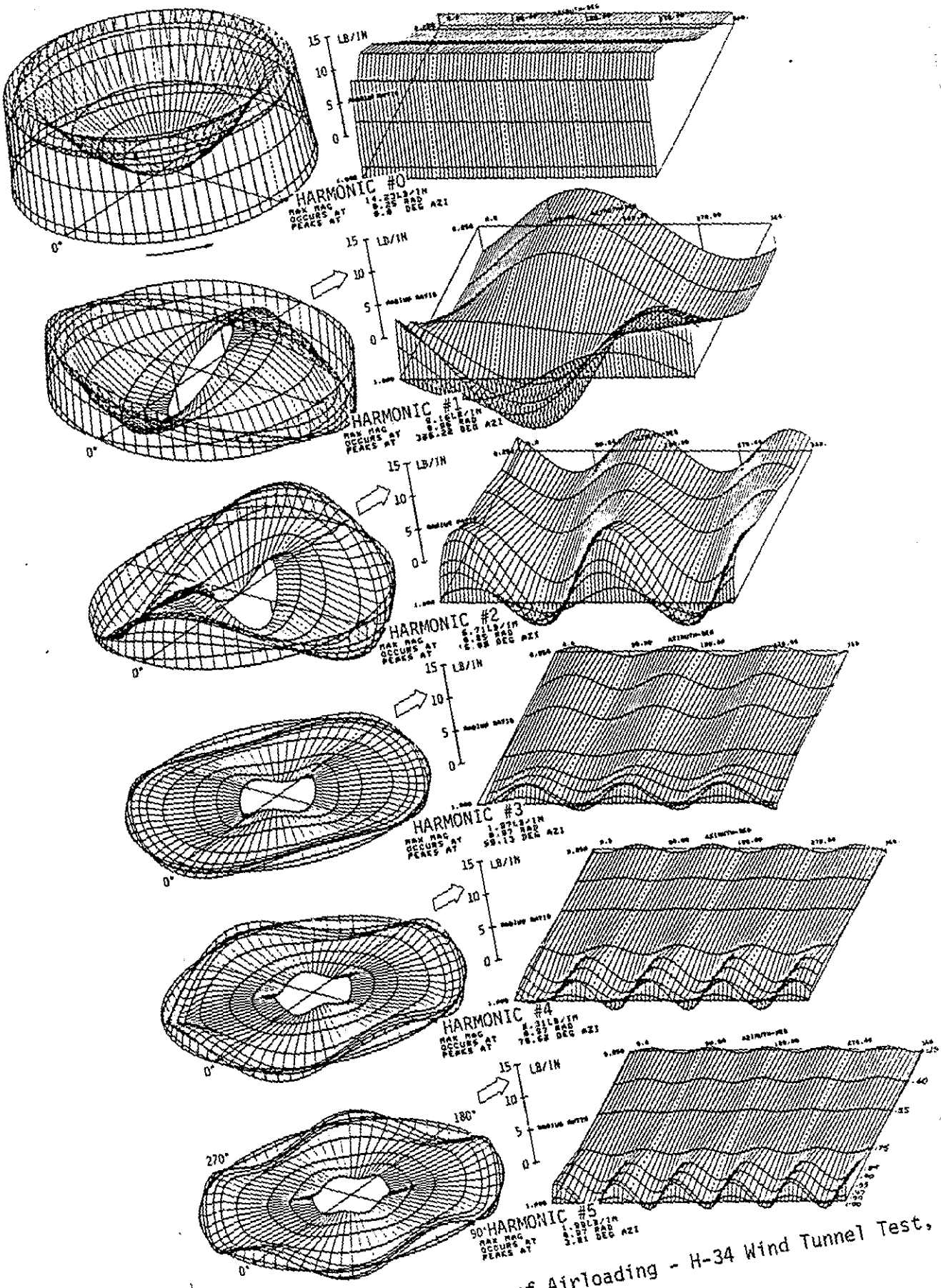

Fig. 3. Harmonic Components of Airloading - H-34 Wind Tunnel Test, 150 KT, Shaft 5° Fwd

This corresponds to the sharp minimum in Figure 2 which in effect forces the higher harmonics to have a minimum at this azimuth.

The next step is based on a suggestion made by Prof. Rene Miller and uses a technique he applied in the Ref. (13) paper. Replot the test data eliminating the constant, 1st and 2nd harmonic components (i.e. retaining all the components (3,4, & 5) that contribute to 4/rev vibration, and a most illuminating result appears. Figure 4 shows that the higher harmonics result from a sharp up-down impulse applied to the blade outboard of the 75% radius in the 1st and 2nd quadrant. Even though approximately equal magnitudes of 3,4 and 5/rev harmonics are present around the disc they all result from this impulsive load on the advancing side and virtually cancel out at all other radii and azimuths, including the reversed-flow region.

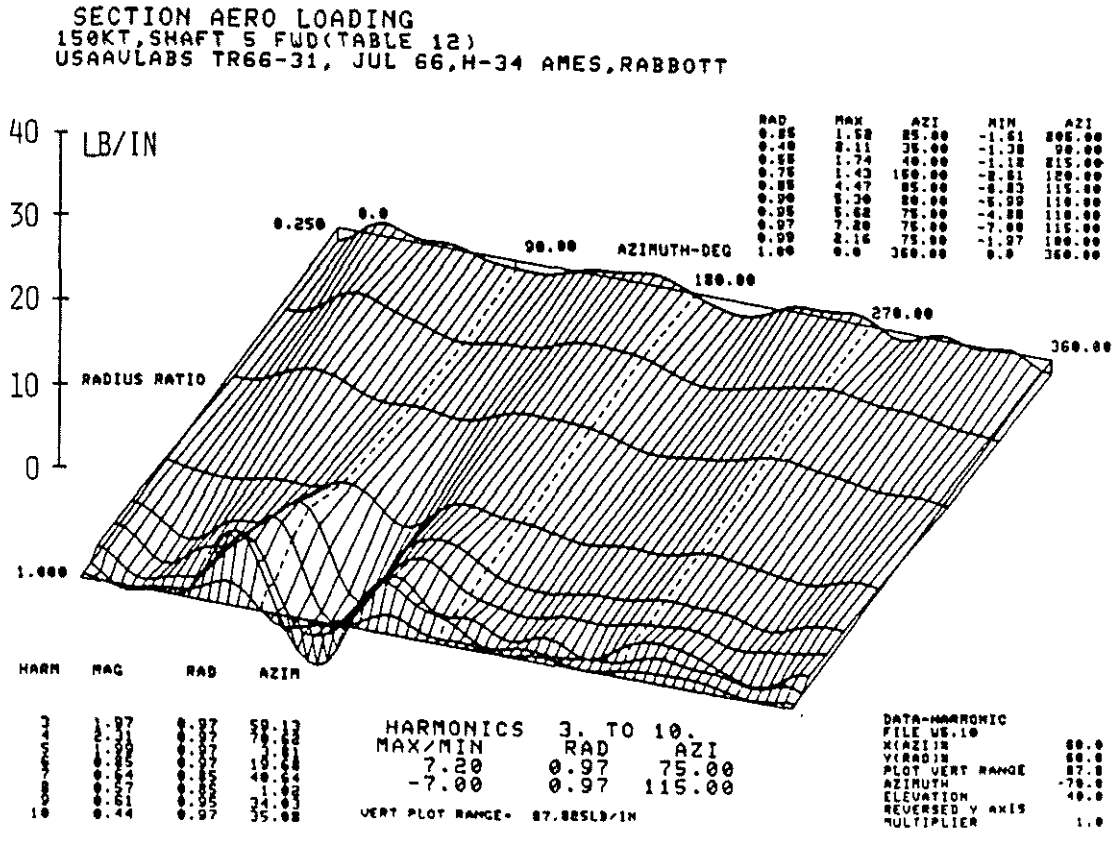

Fig. 4. Harmonics 3 thru 10 of H-34 Airloading

This mode of airload excitation was found to be present to a greater or less extent in almost all the data examined and is thus to a large extent responsible for helicopter n/rev vibration. To convey a clearer impression of the mode of forcing Fig. 5 shows the airloading in the polar format viewed from different azimuths. It is evident that the 'up' region is a ridge extending from the tip at about 75° azimuth and moving rapidly forward with reducing radius. Peaking at about + 7 lb/in and covering about 15% of the radius this represents an 'up-down' impulsive load of about ± 350 lb applied to the tip of the blade. Later this excitation is related to the blade/vortex intersection geometry.

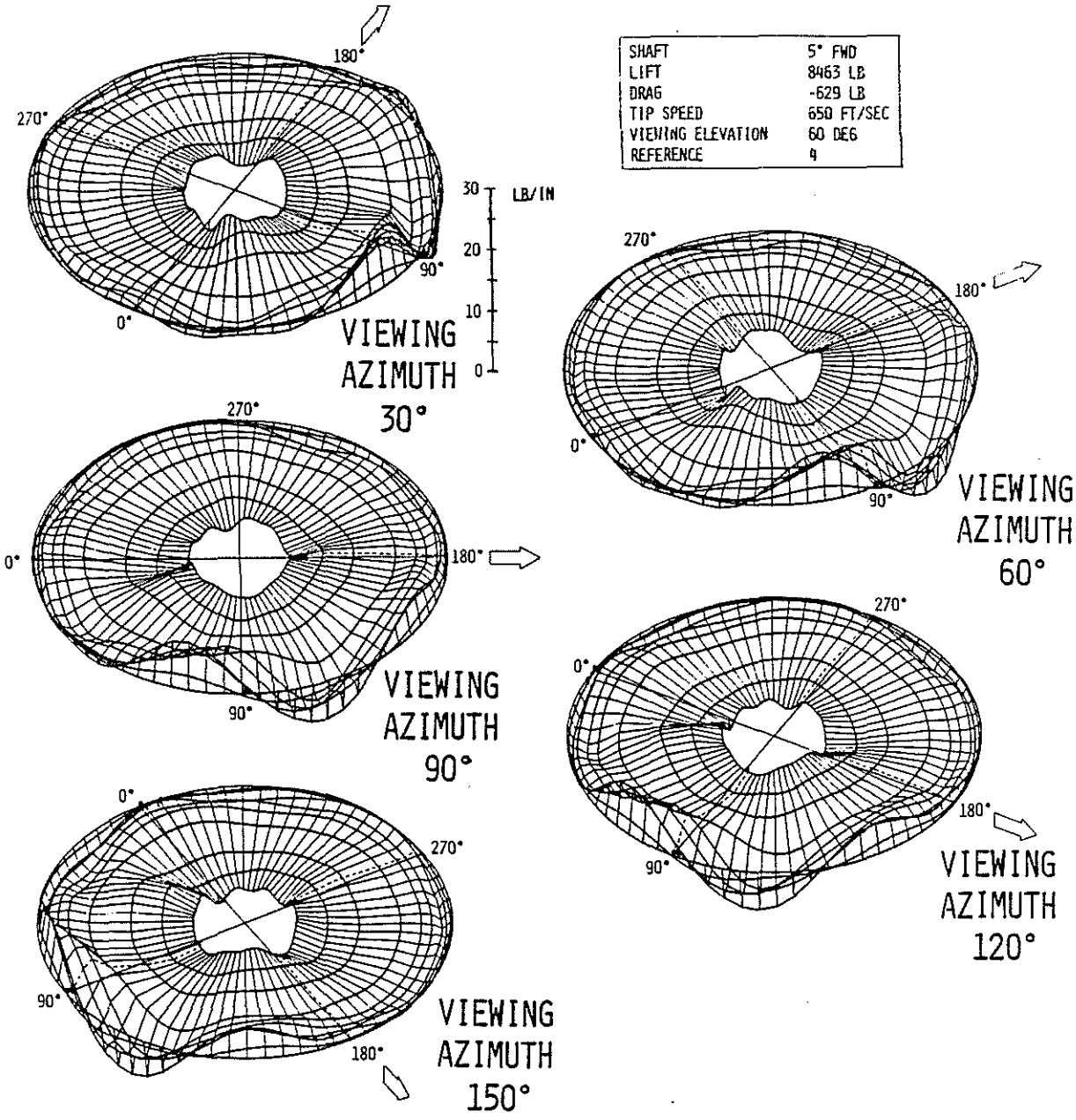

Fig. 5. Harmonics 3 thru 10 of H-34 Airloading at 150 KT - Wind Tunnel Test

3. Flight Conditions

One of the most useful tests for illustrating a wide range of carefully controlled conditions was the H-34 rotor mounted in the Ames 40' x 80' wind tunnel. The test covered 110, 150 and 175 kt with 3 shaft angles varying from 5° fwd thru 0 to 5° aft. In this study every test point was examined in detail using the surface plotting technique, and a few will be shown here to illustrate the more significant conclusions.

Figure 6 shows the effect of tilting the shaft at 150 kt (while using cyclic to maintain zero flapping) and hence changing from a typical helicopter propulsive state to an autorotative state. At first glance the three conditions are surprisingly similar all showing the negative lift in the beginning of the second quadrant, the very low lift in the reverse flow region, and maximum lift regions at the tip in the rear of the disc and inboard at the front of the disc. Examination of the 4th harmonic component shows that while the magnitude increases from 2.31 through 3.05 to 2.60 lb/in with increasingly aft shaft angle, the azimuth at which the 4/rev peaks changes only from azimuth angles of 71° through 77° to 69°. In Figure 7 a comparison is shown of the effect of forward speed from 110 through 175 kt, all at 5° forward shaft angle, and here again the overall shapes are similar although becoming more pronounced at the higher speed. The 4th harmonic airloading increases from 1.85 through 2.31 to 3.76 lb/in while again the azimuth at which the 4th harmonic peaks varies only from 80 to 71 and 71°. Thus an early conclusion of the study noted that while vibratory airloading increases rapidly with forward speed, it reduces as rotor propulsive force is increased, and the phase of the harmonics does not change significantly.

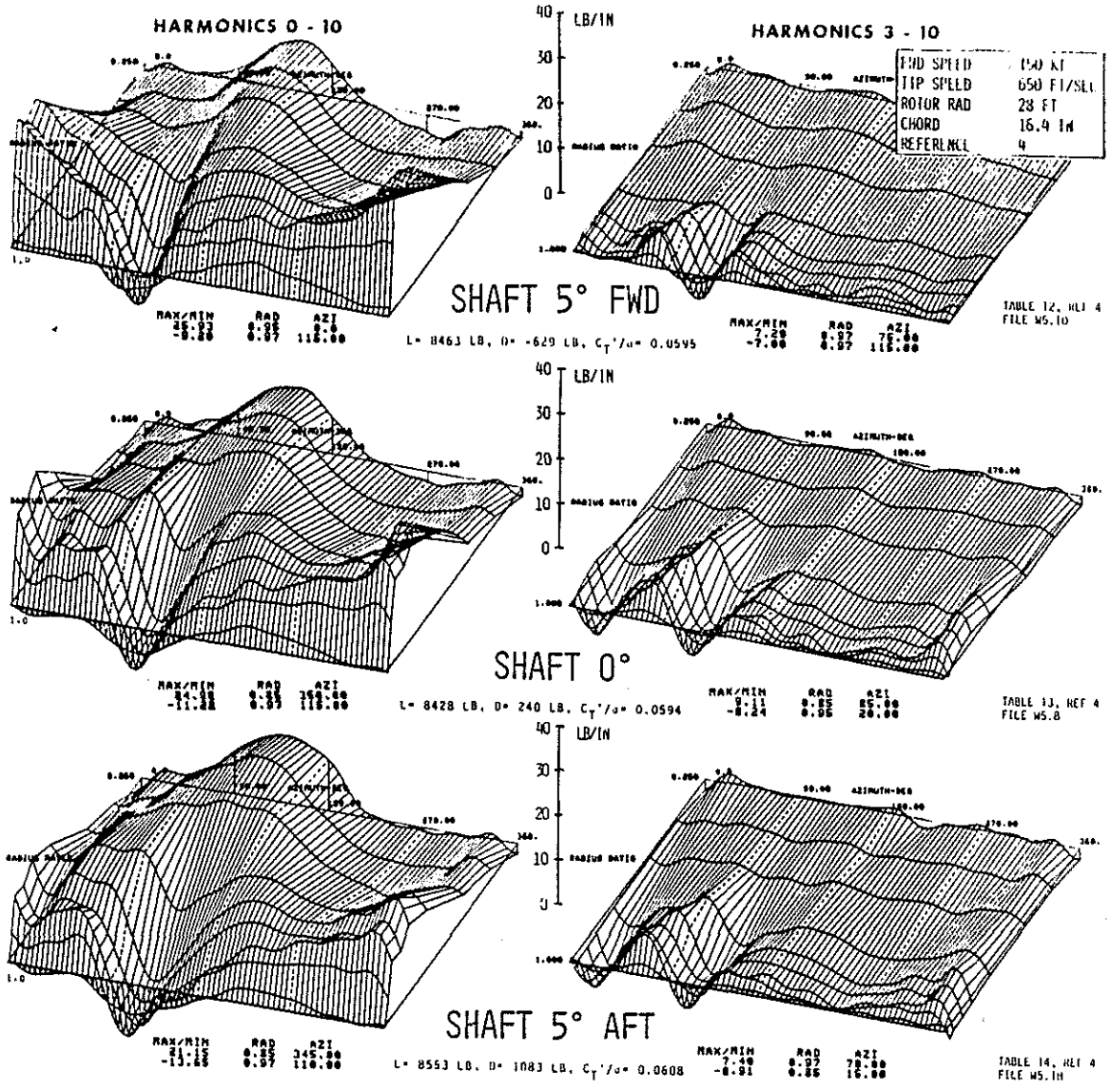

Fig. 6. Effect of Shaft Angle on H-34 Airloading - Wind Tunnel Test

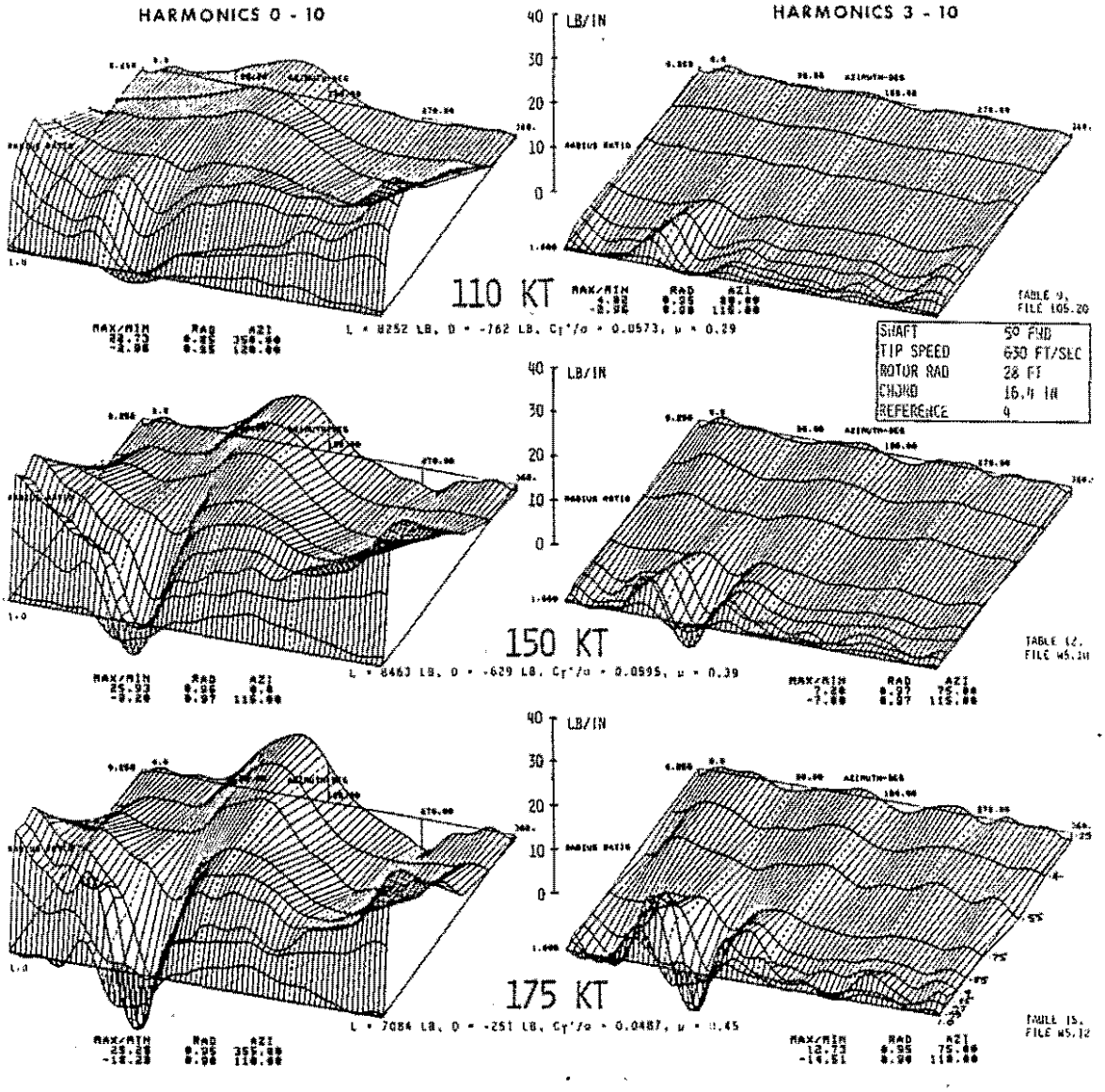

Fig. 7. Effect of Forward Speed on 4-Bladed H-34 Airloading - Wind Tunnel Test

An earlier test program (Ref. 3) on the H-34 gives the airloading in flight test. Level flight data from this program are shown in Fig. 8 from hover to the maximum test speed of 122 kt. Although not as fast as the H-34 wind tunnel test the high speed point shows a similarity to the wind tunnel test data on the advancing side where the principal excitation takes place. In hover the largest excitation occurs at 180° where the blade passes over the tail boom and in the transition speed range 2 regions of excitation occur, one near 90° and the other near 270°.

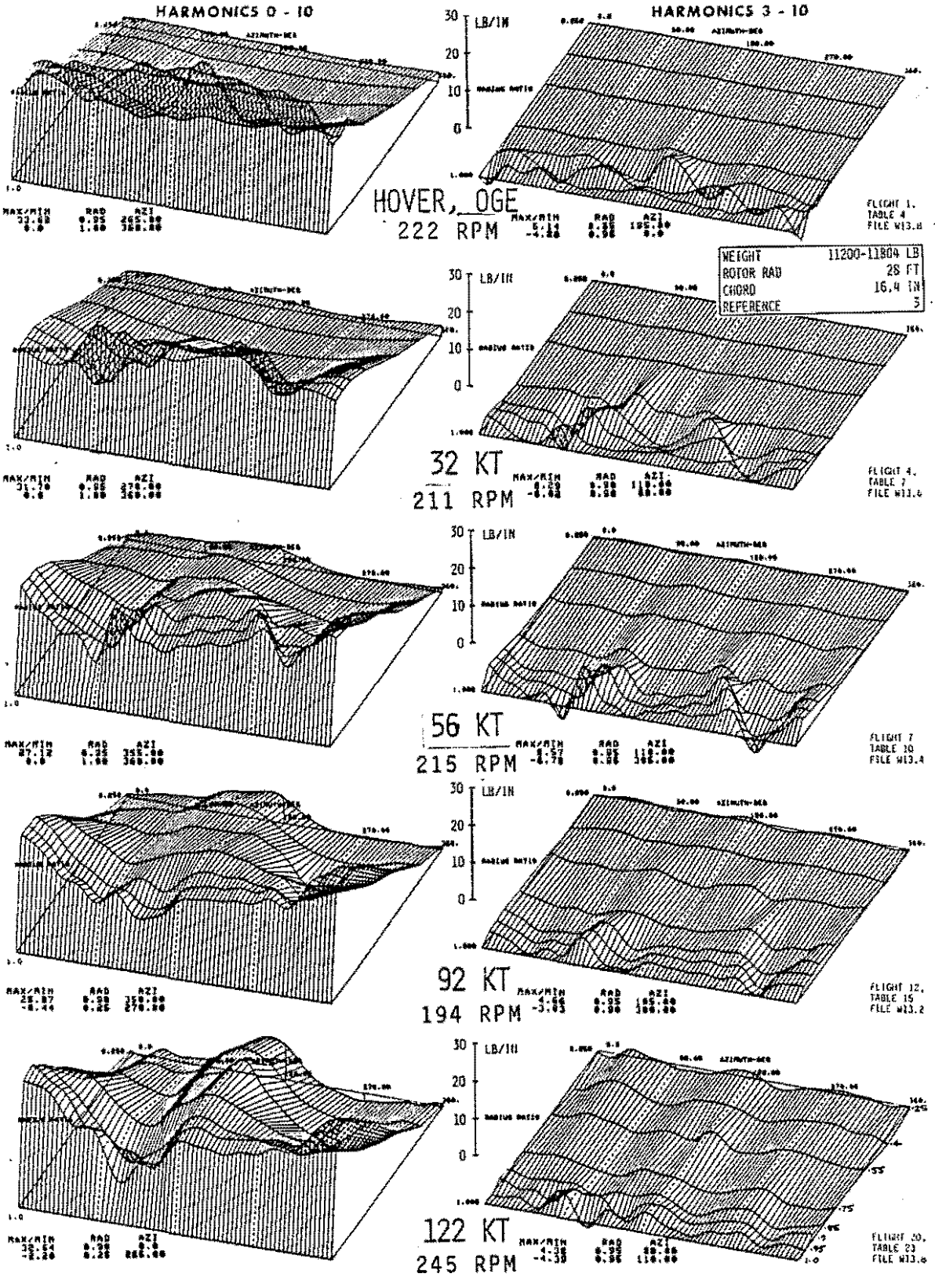

Fig. 8. Effect of Forward Speed on 4-Bladed H-34 Airloading - Flight Test

An even earlier test conducted on a Bell UH-1 is illustrated in Fig. 9 with the only 3 level flight data points recorded. The 33 kt point is strikingly similar to the H-34 56 kt point (Fig. 8) and at 111 kt there is a slight resemblance to the H-34 at the corresponding speed. The maximum values of the impulse loadings all lie between 4 and 5 lb/in.

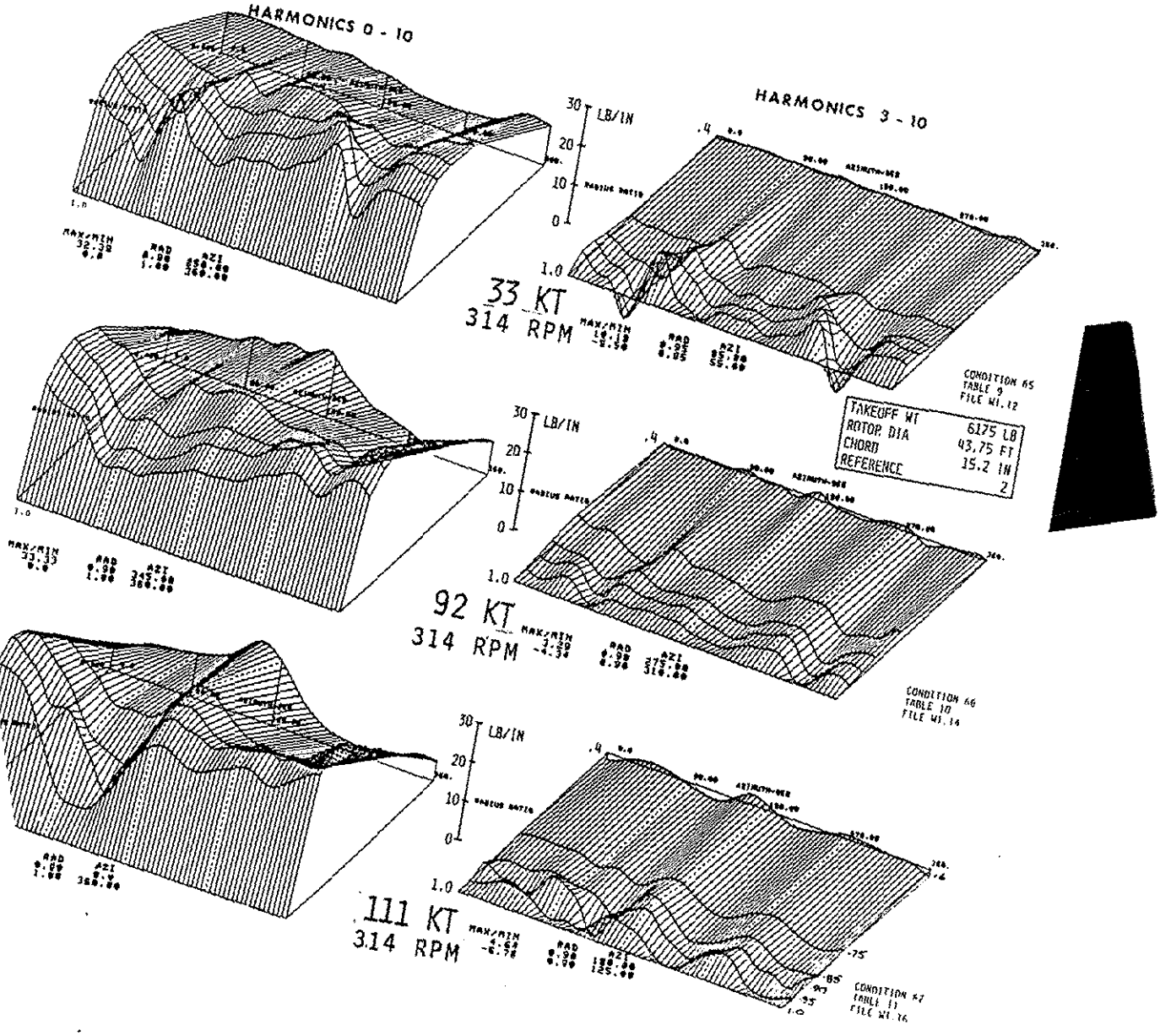

Effect of Forward Speed on 2-Bladed UH-1 Airloading - Flight Test

ent test configuration is shown by the 5 bladed Sikorsky NH-
ion of the S-61) data in Fig. 10. The low speed data aga
es the preceding data and the high speed cases again show t
ion on the advancing side, particularly at the 98% radius
erest is that the 5/rev component of the airloading is

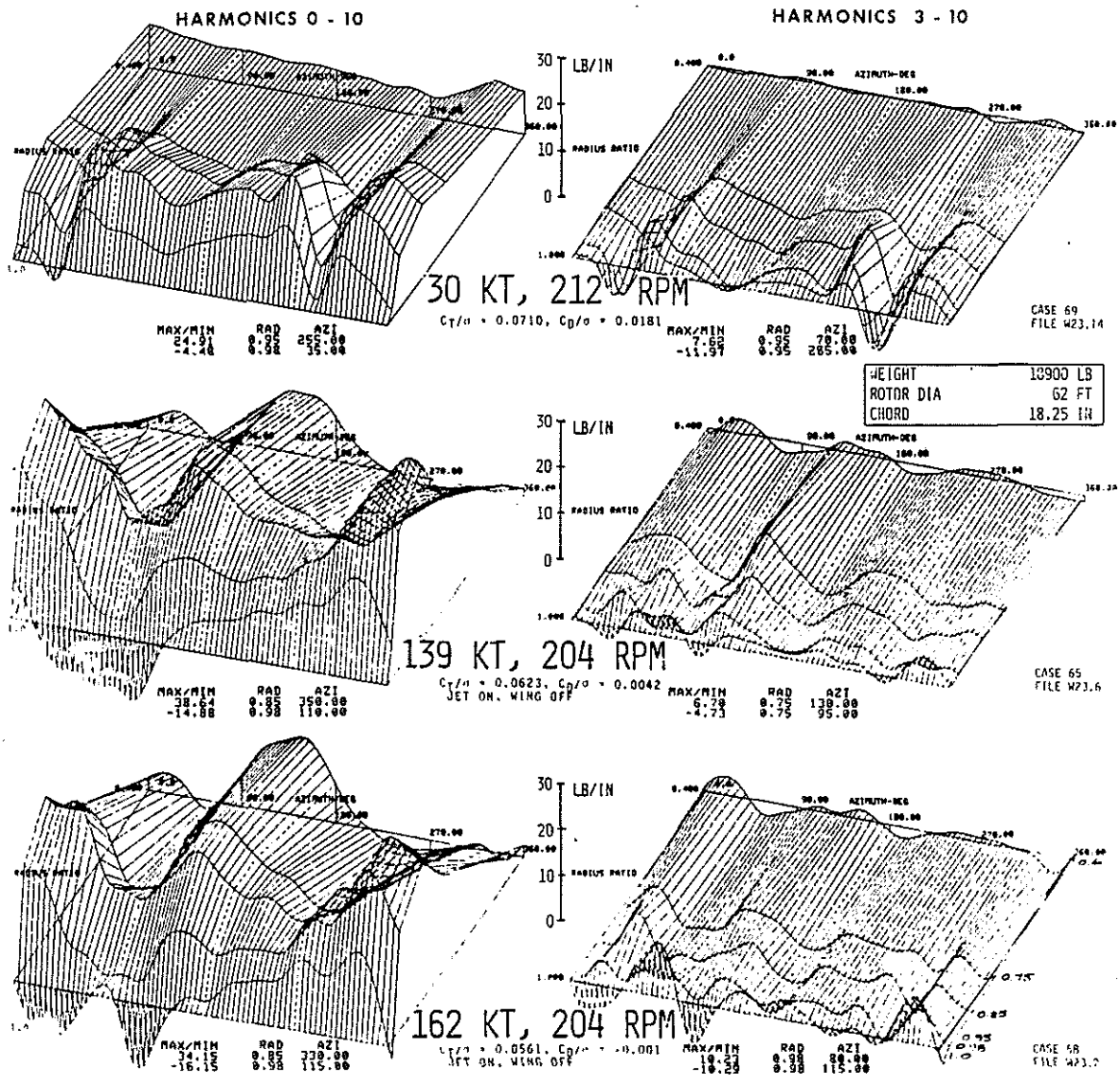

Fig. 10. Effect of Forward Speed on 5-Bladed NH-3A Airloading - Flight Test Ref. 8

accentuated by the 5 bladed rotor. Table 2 shows the maximum harmonics (which all occur near the tip) and, of the vibration causing harmonics, 5 is seen to be the least significant

HARM	30 KT	139 KT	162 KT
3	4.22	2.94	4.91
4	2.78	2.31	4.02
5	1.20	0.71	1.21
6	2.65	0.62	2.39

Table 2. Maximum Airloading Harmonics of the NH-3A (lb/in.)

Data from another compound configuration are provided by the 4 bladed Lockheed XH-51A with level flight speeds up to 227 kt (Fig. 11). Again the low speed results match the preceding data, and at high speed the excitation is again largely on the advancing side at the tip. At 227 kt. the peak response in the first quadrant again clearly occurs at increasing azimuth as radius is reduced from the tip. A secondary small peak also shows the same trend. The transmission on this aircraft was instrumented to measure the Integrated Rotor Load (IRL) and as speed is increased this is seen to reduce as the wing picks up lift and is actually negative at the highest speed.

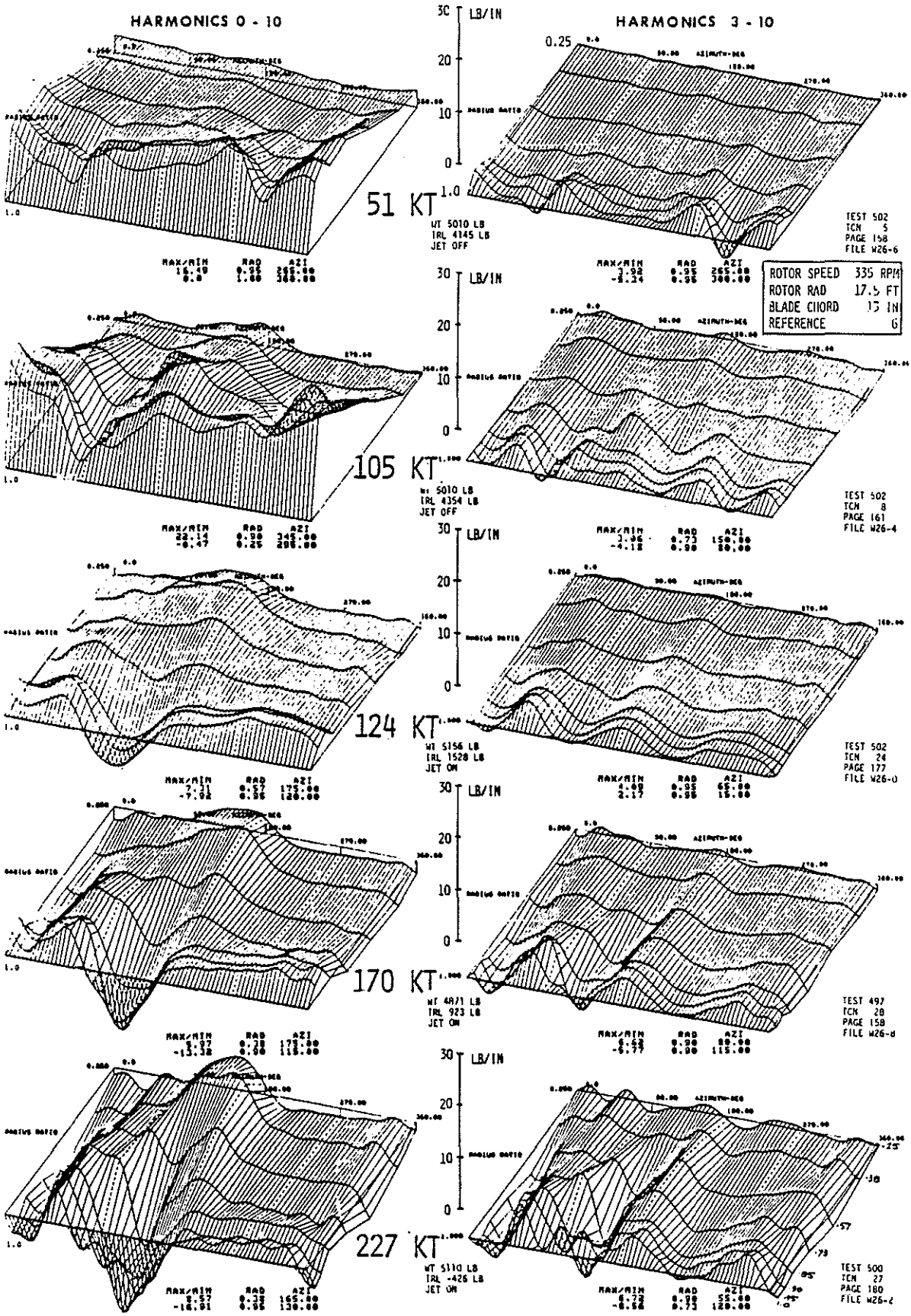

Fig. 11. Effect of Forward Speed on 4-Bladed XH-51A - Flight Test.

More recently a U.S. Navy test program on the Sikorsky CH-53A (ref. 9) provides comprehensive data over a wide range of flight conditions and a representative forward speed sweep is shown in Fig. 12. The characteristic

low speed excitation appears to reach a peak at 63 kt and at high speed, although a sharp excitation is evident at 98% radius, the high frequency excitation is no longer concentrated on the advancing side and in the tip region.

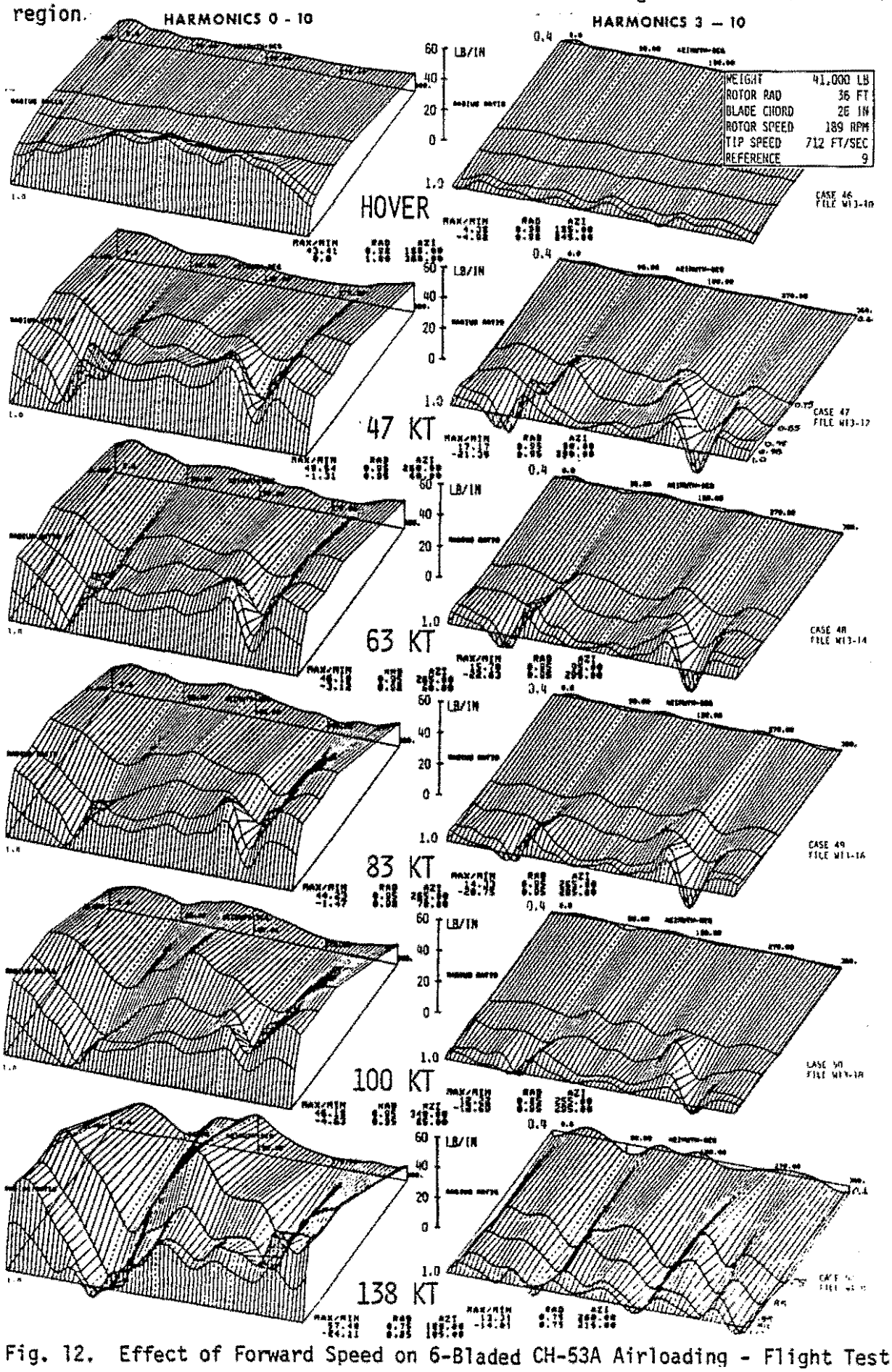

Fig. 12. Effect of Forward Speed on 6-Bladed CH-53A Airloading - Flight Test

The following table of maximum harmonics for the CH-53A show relatively small reductions for harmonics higher than 3rd.

	FORWARD SPEED (KT)					
HARM	0	47	63	83	100	138
3	1.91	7.50	7.82	6.28	3.63	7.14
4	1.21	5.35	4.26	3.45	3.16	3.52
5	1.45	5.35	5.29	5.88	4.58	3.33
6	0.46	4.84	4.18	2.97	1.93	4.84
7	1.24	1.51	1.65	2.88	2.15	1.95

If these airload coefficients are scaled for differing number of blades/rotor they show only small changes in fixed system n/rev vibratory forcing. The 6 bladed rotor is concerned with 6 x the 5, 6 & 7/rev coefficients. A 4 bladed rotor would be concerned with 4 x (6/4) x the 3,4 and 5/rev coefficients. The 6/4 is because a 4 bladed rotor at the same weight would require 50% more chord. Thus the vibratory forcing for rotors with 4, 5 or 6 blades would approximately follow Table 3.

Data from the U.S. Army test of a 2-bladed Bell AH-1G in 1976 are shown in Fig. 13. The lowest speed shown. 72 kt. is probablv past the transition.

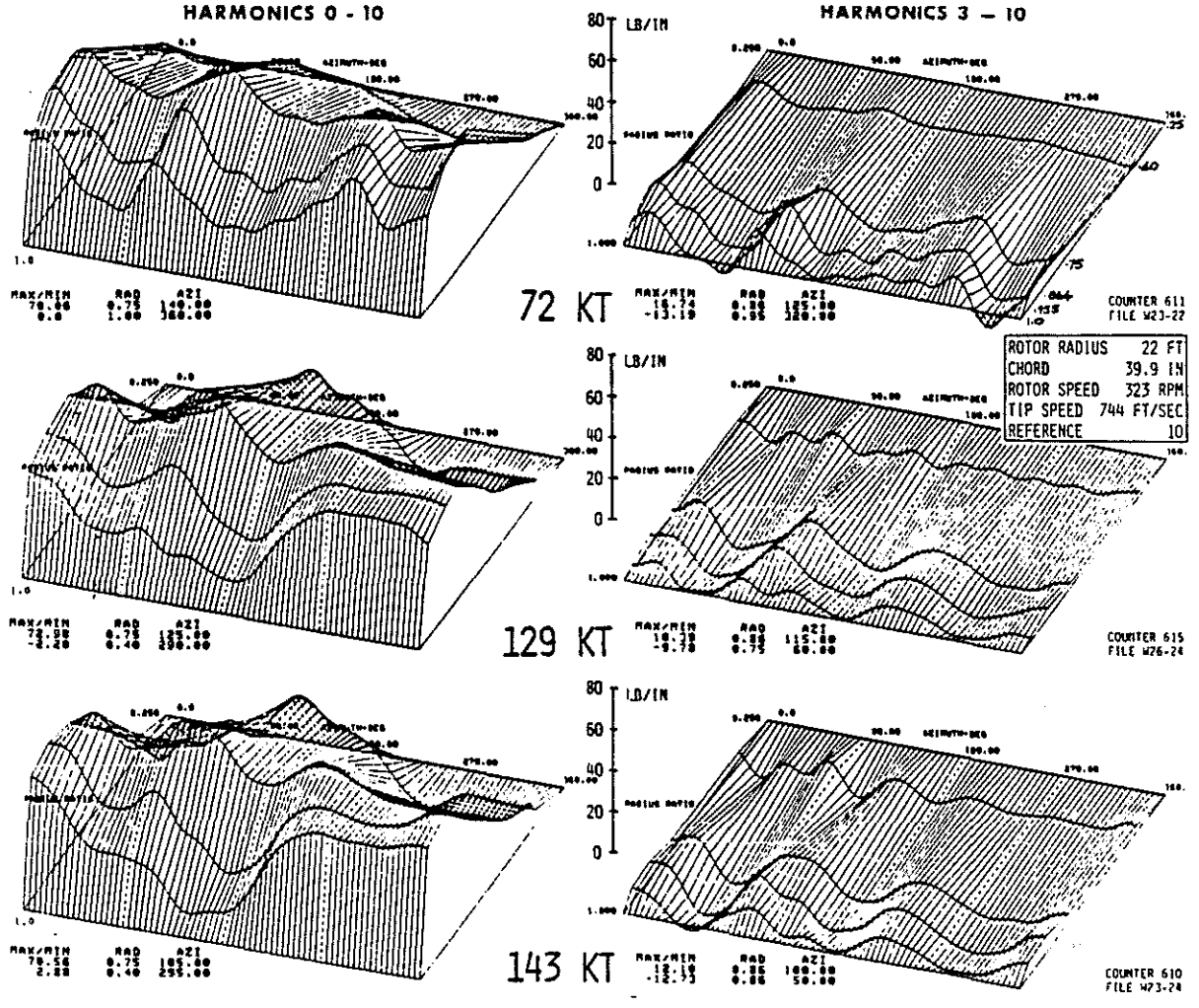

Fig. 13. Effect of Forward Speed on 2-Bladed AH-1G - Flight Tes.

peak but the characteristic peaks on the advancing and retreating sides are seen. At 129 and 143 kt the characteristic ridge on the advancing side is evident but other azimuths also contribute to the excitation. The number of radial stations instrumented for pressures was limited on this program and in 1981 the same aircraft was tested by NASA Ames with 4 more radial stations as well as accelerometer and boundary layer flow instrumentation. Data from this test have not yet been published.

In summary, both the wind tunnel and flight data show some strong similarities in the nature of the airloading which causes vibratory response. In the high vibration transition region the airload distribution for 2 thru 6 bladed helicopters are so similar as to be almost indistinguishable. Every blade gets a strong up-down impulse at the tip on the advancing side followed by a similar but opposite down-up impulse on the retreating side. In the high forward speed regimes similarities are evident but not without exception. Most rotors show:

> one component consisting of an up-down impulse in the first quadrant, increasing in azimuth with reducing radius (Fig. 4)
>
> and a second component appearing as an "up" ridge at 90-120° azimuth, which remains at constant azimuth with reducing radius.

The reversed flow and low q region on the retreating blades consistently show little or no contribution to vibratory airloading.

4. Analytical Modeling

A number of comprehensive rotor analytical methods using rigid wake geometry were used to produce predictions of the airload distribution of the 150 kt, 5 deg. forward shaft case of Fig. 2. To qualify for a thorough correlation study a more rigorous examination of the parametric sensitivities of each method would be needed. However, each analysis was trimmed by collective and cyclic to achieve zero flapping which is close to the actual conditions of the wind tunnel test.

Method (a) in Fig. 14 uses an analysis with a 50 mass representation of the blade. The aerodynamic modelling uses 11 vortices trailed behind the blade for 2 revolutions. Constant lift curve slope is assumed and no corrections are made for Mach No., stall, or tip effects. Method (b) uses 2 flap, and 1 torsion modes and the wake modelling is broken into near, mid and far. The near wake extends for 15° and is compatible with the blade bound circulation. The mid-wake is represented by 13 trailed vortices which extend to 45° behind the blade. The outboard vortices are rolled up using the Betz criterion and the inner vortices are replaced by a single root vortex which together comprise the far wake. Lift calculation method includes 3-D nonlinear, unsteady, compressible aerodynamics. Method (c) used 20 mass stations and a tip and root vortex wake model that extends for about 2 revolutions. Lift is determined in the same manner as method (b). Method (d) is described in ref. 12 and uses 50 masses and also near, mid and far wake modelling. Lift calculations also use lifting line theory and steady 2D airfoil characteristics with corrections for unsteady and 3D flow effects.

All the methods show general agreement with the full 0-10 harmonics. However, none of the methods is successful in achieving a close match with the vibratory 3-10 harmonic data. There are encouraging indications in the results of the necessary mechanisms, but clearly all methods require improvement before becoming useful design tools for reducing vibratory airloading.

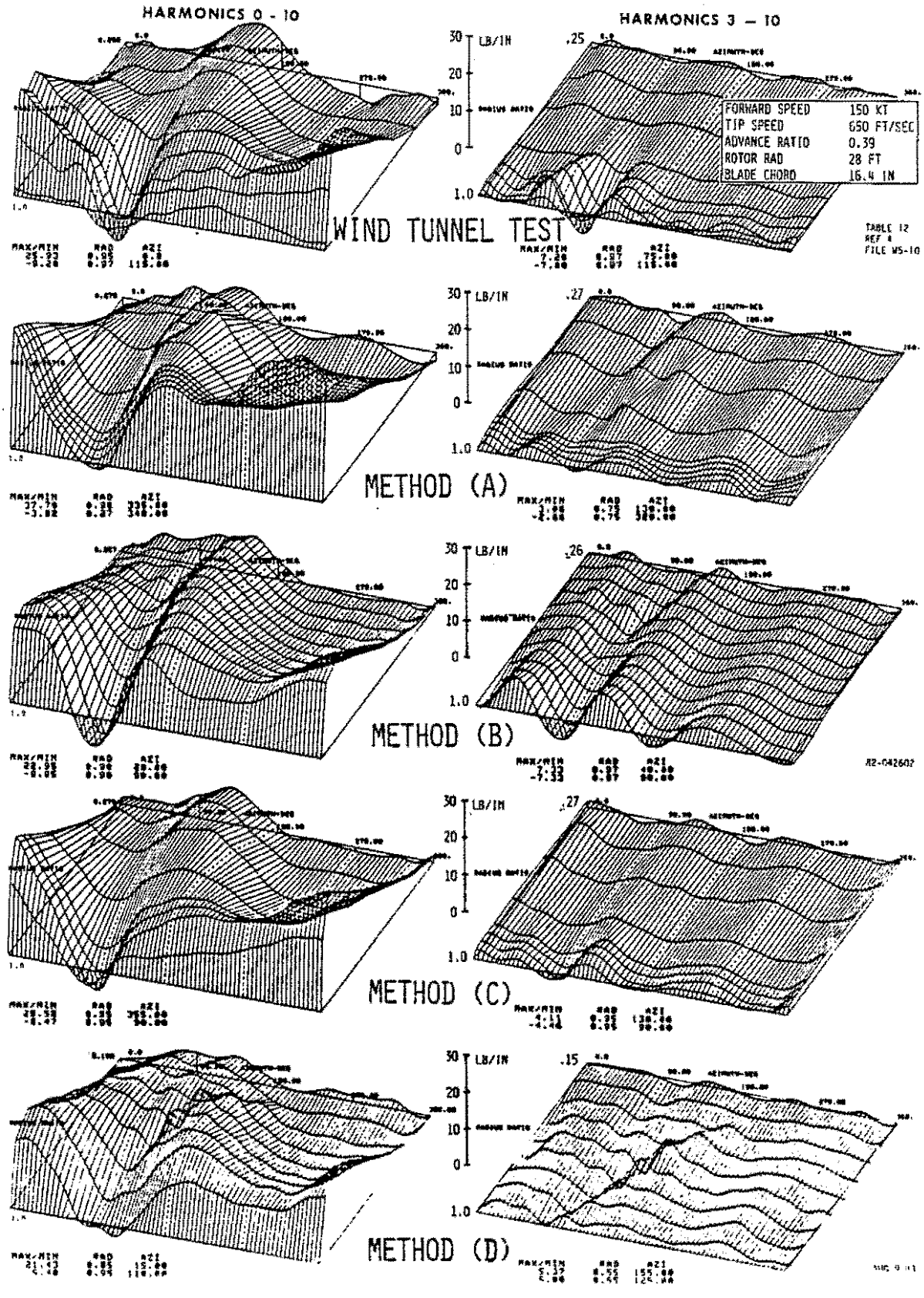

Fig. 14. Correlation of Analytical Predictions of Airloading - H-34 Wind Tunnel Test, 150 KT, Shaft 5° Forward

Are the impulsive airloadings caused by blade-vortex interactions? At the top of Fig. 15 test data are shown for the H-34 at 56 and 150 kt. The next

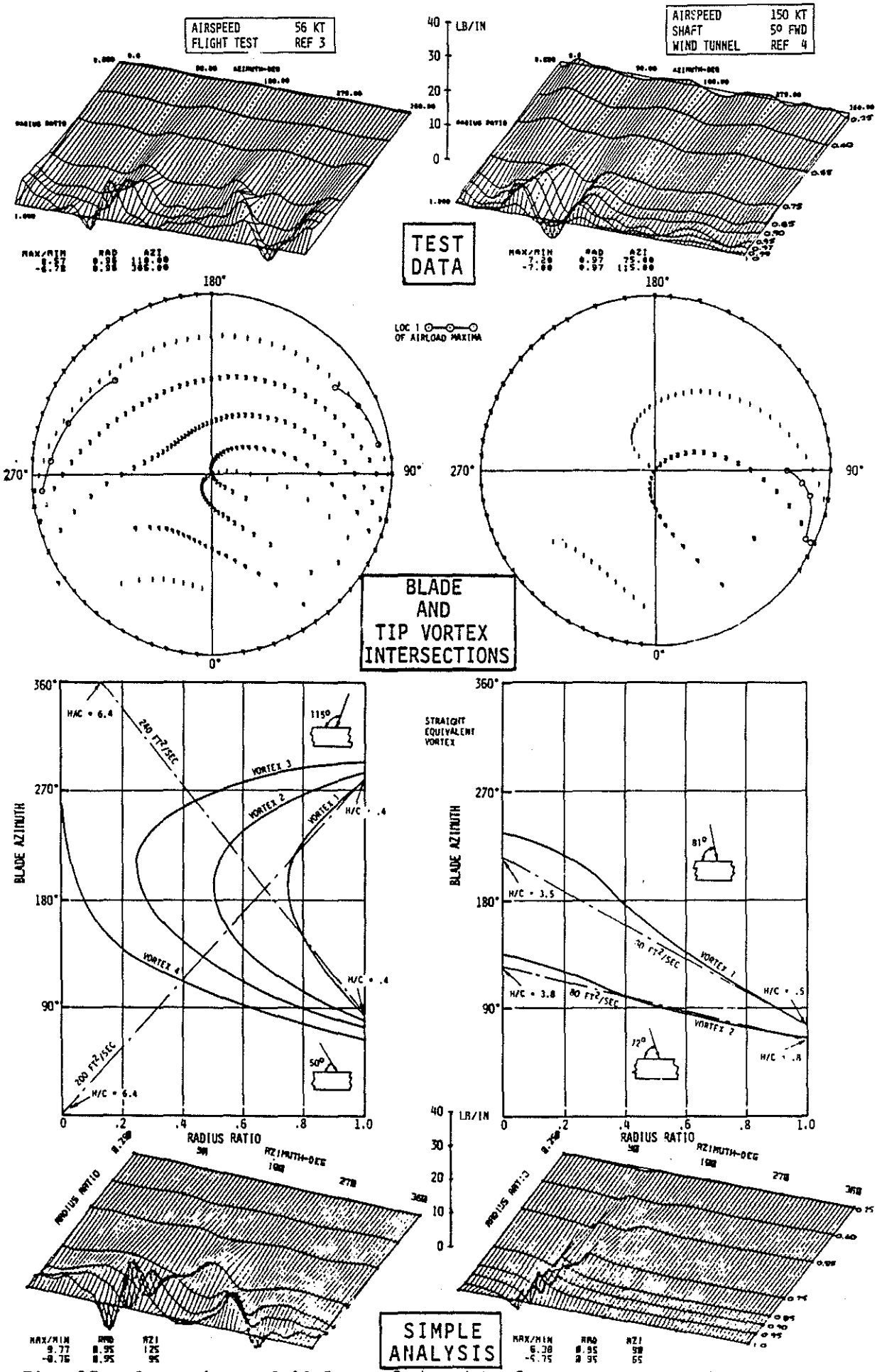

Fig. 15. Comparison of Airloads Induced by Intersection of Blades and Tip Vortices With H-34 Test Airloading (Harmonics 3 thru 10)

diagram down shows a plan view of the loci of intersection between blades and their preceding tip loci (e.g. points marked 1 show the locus of intersections between a blade and the tip locus trailed from 1 blade spacing ahead, etc.). The interconnected circled points show the locus of the maxima from the test data above. Clearly, there is a striking correlation at both low and high speeds.

The next diagram is a linear development of the circular plot. Using this visualization a simple analytical model is constructed consisting of a wing passing over an infinite straight vortex with varying vertical separation, and inclined to the blade as shown. The lower plot shows the resultant loads predicted from the wing passing over the vortices. The agreement at low speed is good enough to suggest that this mechanism contains the essentials for a more thorough prediction of the vibratory airload. At high speed however, the agreement is poor, mainly because the impulse has the wrong sign, i.e. an intersection on the advancing side with a vortex resulting from a lifting preceding blade necessarily produces a 'down-up' impulse as in the low speed case. An implication could be that significant vorticity of the opposite direction is produced on the advancing side by the negative lift region at the tip at high speed.

5. Conclusions

The vibratory components of the airloading that cause helicopter vibration are surprisingly consistent despite substantial differences in size, trim and numbers of blades per rotor.

At transition speeds where vibration usually reaches a peak the vibratory airloading appears to be almost entirely due to the interaction between blades and the vortices trailed from the preceding blades. This results in a sharp 'down-up' impulse being applied to the tip of the advancing blade and an opposite impulse being applied to the tip of the retreating blade.

At high forward speeds the blade loading is more variable but similarities are still evident. The advancing blade tip is usually the most heavily loaded and the mode of forcing is related to the intersection of the blade and the tip vortex from the preceding blade.

Acknowledgements

My thanks are due to Jonathan Grace, Jim McLaughlin, and Bill Hardy for their invaluable assistance in data processing techniques. Also to Nick Dorofee and Ken Bartie for their help in assembling this paper.

References

1. Rabbott, J. P. & Churchill, G. B., "Experimental Investigation of the Aerodynamic Loading on a Helicopter Rotor Blade in Forward Flight." NACA RM L56I07, Oct. 1956.

2. Bell Helicopter, "Measurement of Dynamic Air Loads on a Full-Scale Semi-Rigid Rotor" TCREC TR 62-42. Dec. 1962.

3. Scheiman, J., "A Tabulation of Helicopter Rotor-Blade Differential Pressures, Stresses, and Motions as Measured in Flight." NASA TM X-952. Mar. 1964.

4. Rabbott, J. P., Lizak, A. A., & Paglino, V. M., "A Presentation of Measured and Calculated Full-Scale Rotor Blade Aerodynamic and Structural Loads." USAAVLABS TR66-31, Jul. 1966.

5. Pruyn, R. R., "In-Flight Measurement of Rotor Blade Airloads, Bending Moments, and Motions, Together with Rotor Shaft Loads and Fuselage Vibration, on a Tandem Rotor Helicopter." USAAVLABS TR 67-9A, B, C & D, Nov. 1967.

6. Bartsch, E. A., "In-Flight Measurement and Correlation with Theory of Blade Airloads and Resources in the XH-51A Compound Helicopter Rotor." USAAVLABS TR 68-22A. May 1968.

8. Fenaughty, R. & Beno, E., "NH-3A Vibratory Airloads and Vibratory Rotor Loads." Department of the Navy SER 611493. Jan 1970.

9. Beno, E., "CH-53A Main Rotor and Stabilizer Vibratory Airloads and Forces." Department of the Navy SER 65593. Jun 1970.

10. Shockey, G. A., Cox, C. Z., Williams, J. W., "AH-1G Helicopter Aerodynamic and Structural Load Survey." USAAMRDL TR-76-39.

11. Shockey, G. A., et al, "AH-1G Tip Aero-Acoustic Test." NASA (to be published).

12. Johnson, W., "Development of a Comprehensive Analysis for Rotorcraft-I. Rotor Model and Wake Analysis." VERTICA Vol. 5, P99-129, 1981.

13. Miller, R. H., "Unsteady Air Loads on Helicopter Rotor Blades." The Fourth Cierva Memorial Lecture, Rotorcraft Section, Journal of the Royal Aeronautical Society, April 1964.